Published in final edited form as:
Cell Calcium. 2009 July ; 46(1): 73–84. doi:10.1016/j.ceca.2009.05.003.

Reduction in TRPC4 expression specifically attenuates G-protein coupled receptor-stimulated increases in intracellular calcium in human myometrial cells

Aida Ulloa[1,2], **Albert L. Gonzales**[1,3], **Miao Zhong**[1,*], **Yoon-Sun Kim**[1], **Jeremy Cantlon**[1], **Colin Clay**[1,2], **Chun-Ying Ku**[1], **Scott Earley**[1,2,3], and **Barbara M. Sanborn**[1,2,4]

[1]Department of Biomedical Sciences, Colorado State University, Fort Collins, CO

[2]Cell and Molecular Biology Program, Colorado State University, Fort Collins, CO

[3]Molecular and Cellular Integrative Neuroscience Program, Colorado State University, Fort Collins, CO

Abstract

Canonical transient receptor potential (TRPC) proteins may play a role in regulating changes in intracellular calcium ($[Ca^{2+}]_i$). Human myometrium expresses TRPC4, TRPC1 and TRPC6 mRNAs in greatest relative abundance. Contributions of TRPC4 to increases in $[Ca^{2+}]_i$ were assessed in PHM1-41 and primary human uterine smooth muscle (UtSMC) cells using short hairpin RNAs (shRNAs). Based on a reporter assay screen, one shRNA was selected to construct an adenoviral expression vector (TC4sh1). TC4sh1 induced both mRNA and protein TRPC4 knockdown in PHM1-41 cells without affecting expression of other TRPCs. Signal-regulated Ca^{2+} entry (SRCE), defined as a stimulus- and extracellular Ca^{2+}-dependent increase in $[Ca^{2+}]_i$, was measured in PHM1-41 cells treated with oxytocin (G-protein coupled receptor (GPCR)-stimulated), thapsigargin (store depletion-simulated), and OAG (diacylglycerol-stimulated), using Fura-2. Cells infected with TC4sh1 exhibited attenuated oxytocin-, ATP- and PGF2α–mediated SRCE, but no change in thapsigargin- or OAG-stimulated SRCE. Similar results were obtained in primary uterine smooth muscle cells. Additionally, cells expressing TC4sh1 exhibited a significantly smaller increase in channel activity in response to oxytocin administration than did cells infected with empty virus. These data show that, in human myometrial cells, knockdown of endogenous TRPC4 specifically attenuates GPCR-stimulated, but not thapsigargin- or OAG-stimulated extracellular calcium-dependent increases in $[Ca^{2+}]_i$. These data imply that, in this cellular context, the mechanisms regulating extracellular Ca^{2+}-dependent increases in $[Ca^{2+}]_i$ are differentially affected by different signaling pathways.

1. Introduction

Ca^{2+} signaling is achieved as a result of increases in the concentration of intracellular free Ca^{2+} ($[Ca^{2+}]_i$). The myometrium, the smooth muscle of the uterine wall, is responsible for

4To whom inquiries should be sent: Dr. B. M. Sanborn, Department of Biomedical Sciences, Colorado State University, 1680 Campus Delivery, Fort Collins, CO 80523-1680, Ph 970-491-4263, Fax 970-491-3557, Barbara.Sanborn@colostate.edu.
*Current address: Center for Cancer Research and Therapeutic Development, Clark Atlanta University, 223 James P Brawley Drive SW, Atlanta, GA 30314

maintaining a secure environment for the developing fetus during pregnancy and for the expulsive uterine contractions of labor. Increases in $[Ca^{2+}]_i$ correlate with increases in myosin light chain phosphorylation and with increases in tension [1].

Activation of receptors and/or depletion of agonist-sensitive intracellular Ca^{2+} stores stimulate Ca^{2+}-uptake from the extracellular environment. Stimulation of G-protein coupled receptors (GPCRs) and receptor tyrosine kinases activate phospholipases C (PLCs), which can induce hydrolysis of phosphatidylinositol bisphosphate to produce inositol-(1,4,5) triphosphate (IP_3) and 1,2-diacylglycerol. IP_3 binds to and activates the IP_3 receptors (IP_3-Rs) in the endoplasmic reticulum (ER), resulting in Ca^{2+} release from these intracellular stores. Receptor-operated Ca^{2+} entry from the extracellular environment can be achieved by mechanisms that are dependent or independent of intracellular Ca^{2+} store depletion [2]. Store depletion can also induce extracellular Ca^{2+} entry through several mechanisms (reviewed in [2-4]). For simplicity, receptor- and store-operated Ca^{2+} entry mechanisms, as well as those activated by other second messengers, measured as stimulus- and extracellular Ca^{2+}-dependent increases in $[Ca^{2+}]_i$, are operationally referred to in the present study as signal-regulated Ca^{2+} entry (SRCE).

The canonical type of transient receptor potential (TRPC) proteins are candidates for SRCE channels. Characteristics of these channels range from cation nonselectivity, where both mono- and divalent ions can carry inward currents, to channels exhibiting high Ca^{2+} selectivity [2]. Stimuli such as GPCR-activation, IP_3-R activation, inhibition of endoplasmic reticulum Ca^{2+}-ATPase (SERCA) pumps resulting in endoplasmic reticulum Ca^{2+} store depletion, and diacylglycerol itself have all been implicated in inducing TRPC activation directly or indirectly [2,3].

The TRPC1-7 isoform expression profile can vary dramatically from one cell type to another as well as among the same cell types in different organisms. The tetrameric nature of the channel and the differential expression of specific TRPCs create the possibility of cell-specific homo- or heterotetrameric channels with unique functional properties [5]. As a result of interaction domains in both N- and C-termini, each TRPC subunit forming the channel can potentially contribute to the formation of macromolecular complexes unique to specific cell types [2]. The functional and regulatory properties of these potentially unique endogenous TRPC homo- and/or heterotetramer channels are still unknown.

Human pregnant myometrial tissue, primary human myometrial cells and PHM1-41 cells all express TRPCs except TRPC 2 (a pseudogene in humans) [6-9]. TRPC4, TRPC1 and TRPC6 mRNAs are present in higher relative abundance than TRPC3, TRPC5 and TRPC7 mRNAs [9]. TRPC1, 3, 4 and 6 proteins have been detected by immunoblot in human myometrial cells and tissue [6-9]. PHM1-41 immortalized human myometrial cells exhibit SRCE in response to oxytocin, thapsigargin and OAG [6,10-13], but the involvement of specific TRPCs in one or more of these responses has not been determined to date. Even though voltage-operated Ca^{2+} entry plays an important role in regulating myometrial contractions [14,15], PHM1-41 cells exhibit minimal response to depolarization with KCl [6], and oxytocin- and thapsigargin-mediated SRCE is nifedipine-independent [12,16].

In this study the specific role of TRPC4 in myometrial SRCE was investigated using RNA interference (RNAi). Because we have found that PHM1-41 and primary human uterine smooth muscle (UtSMC) cells are difficult to transfect efficiently, we constructed an adenoviral vector expressing a TRPC4 short hairpin RNA (shRNA) construct to achieve specific TRPC4 knockdown. The data indicate that attenuation of TRPC4 expression specifically induces a decrease in GPCR-stimulated, but not in thapsigargin- or OAG-stimulated increases in $[Ca^{2+}]_i$ in myometrial cells.

2. Materials and methods

2.1 Reagents and solutions

Primers were purchased from Integrated DNA Technologies, Inc (Coralville, IA). SYBR Green I nucleic acid gel stain was purchased from Lonza (Rockland, ME). Restriction enzymes were obtained from New England Biolabs Inc. (Beverly, MA) or Promega (Madison, WI). Fura-2/acetoxymethylester (Fura 2-AM) and Pluronic F127 were obtained from Molecular Probes (Invitrogen, Carlsbad, CA). Oxytocin, thapsigargin, ATP, Prostaglandin F (PGF)2α and protease inhibitor cocktail were purchased from Sigma-Aldrich (St. Louis, MO). 1-oleoyl-2-acetyl-*sn*-glycerol (OAG) was obtained from Calbiochem (San Diego, CA). Cell culture media and other reagents were obtained from Gibco BRL Invitrogen (Carlsbad, CA). TRPC1 rabbit monoclonal antibody and its corresponding blocking peptide were obtained from Epitomics (Burlingame, CA). TRPC4 polyclonal antibody and its corresponding blocking peptide were purchased from Alomone Labs (Jerusalem, Israel). Anti-HA peroxidase mouse monoclonal antibody was purchased from Roche (Indianapolis, IN). Primary polyclonal human PLCB3 antibody and horseradish peroxidase (HRP) conjugated donkey anti-rabbit secondary antibodies were purchased from Santa Cruz Biotechnology Inc. (Santa Cruz, CA)

2.2 Cell Culture

UtSMC cells derived from nonpregnant human myometrium (Catalog #: CC-2562 Lot # 17590) were purchased from Lonza (Walkersville, MD). AD293 cells were obtained from Stratagene (La Jolla, CA). UtSMC and AD293 cells were cultured in Dulbecco's Modified Eagle Medium (DMEM) containing 10% fetal calf serum, 2 mM L-glutamine, 50 units/ml penicillin, and 50 μg/ml streptomycin. Immortalized PHM1-41 cells were derived from late-term pregnant human myometrial tissue and retain many morphological and biological characteristics of myometrial smooth muscle cells [10,12,17-19]. PHM1-41 cells were cultured in the media described above including 0.1 mg/ml of G418 sulfate (Gibco BRL Invitrogen, Carlsbad, CA PHM1-41 cells were used at passages 20-25 and UtSMC were used at passages 6-10. Myometrial cells were trypsinized and plated in 35 mm glass-bottomed dishes (MatTek, Ashland, MA) for Ca^{2+}-imaging experiments or into 100-mm dishes for RT-qPCR and immunoblot studies.

2.3 Cloning, adenovirus construction and adenoviral infection

Full-length human TRPC4 alpha cDNA in pcDNA3 was obtained from Dr. J.W. Putney, Jr. (NIEHS, Raleigh NC). The TRPC4 luciferase reporter (psiTC4) vector was constructed by introducing a NotI restriction site by polymerase chain reaction (PCR) at each end of the TRPC4 cDNA sequence using the Expand High Fidelity PLUS PCR System (Roche Applied Science, Indianapolis, IN); the resulting product was cloned into the NotI site of the psiCHECK-2 vector (Promega, Madison, WI).

TRPC4 shRNAs were designed using the Dharmacon siDesign Center (Lafayette, CO). Sequences were examined for features indicating siRNA functionality [20]. Candidate sequences homologous to other TRPCs, other ion channels and common interaction domains were rejected. Selected siRNA duplex sequences were constructed to contain a human pre-microRNA stem sequence (miR-30) which allows efficient processing of the shRNA [21]. A scrambled control sequence was designed by entering the TRPC4-shRNA#4 sequence into the siRNA Sequence Scrambler software (GenScript, Piscataway, NJ). Oligonucleotides containing TRPC4-shRNA sequences were synthesized (Integrated DNA Technologies, Coralville, IA) and cloned into the BseRI and BamHI sites downstream of a U6 promoter in the pSHAG vector (provided by G. Hannon, Cold Spring Harbor Laboratory, NY), producing the pSH-TC4sh1-4 vectors.

A modified pAdTrack-RfA(f) plasmid was constructed by introduction of the Reading Frame Cassette A (RfA) from the Gateway Vector Conversion System (Invitrogen, Carlsbad, CA) into the XbaI/XhoI restriction sites in pAdTrack (ATCC, Manassas, VA). TRPC4 shRNA adenoviral vector assembly was performed by recombination between the *attR* sites of pSH-TC4sh1 and the *attL* sites of pAdTrack-RfA(f) using LR clonase. The pAdT-TC4shRNA clones were checked by restriction enzyme digestion and sequence integrity was confirmed by direct sequencing. The pAdT-TC4shRNA clones were linearized with PmeI and subsequently electroporated into *Escherichia coli* BJ5183 cells according to the manufacturer's instructions to achieve recombination of the pAdT-TC4shRNAs with the adenoviral backbone plasmid pAdEasy-1 (Stratagene, La Jolla, CA). The obtained recombined plasmids were linearized with PacI and transfected into AD-293 cells to allow viral synthesis and packaging. The adenoviruses were amplified, purified using the BD Adeno-X Maxi Purification kit (Clontech, Mountain View, CA), and titered by viral particle titration and end-point dilution. Adenoviruses were then used to infect PHM1-41 cells, using the enhanced green fluorescent protein (eGFP) marker to identify infected cells. Multiplicity of infection (MOI) of 1000 and 500 were used in PHM1-41 and UtSMC cells respectively, resulting in 90-95% infection efficiency as determined by eGFP expression. Cells were used within 72-96 h post-infection and exhibited morphology similar to that of noninfected cells, as determined by visual inspection.

2.4 Transfection and electroporation

AD293 cells were plated at 1×10^5 cells/well in 12-well plates. Transient transfections were performed 24 h after plating using the GenePORTER2 transfection reagent according to the manufacturer's instructions (Genlantis, San Diego, CA). Cells were cotransfected with the psiTC4 reporter and the pSH-TC4sh1-4 constructs at a 1:3 molar ratio. Samples were analyzed 48-72 hours post-transfection using the Dual-luciferase Reporter Assay (Promega, Madison, WI).

COSM6 cells were plated at 1×10^5 cells/well in 6-well plates. Transient transfections were performed 24 h after plating using the FuGENE 6 transfection reagent (Roche, Indianapolis, IN) according to manufacturer's instructions. Cells were cotransfected with the TRPC4 overexpression plasmid and the pSH-TC4sh1 construct at a 1:3 molar ratio. Samples were analyzed 72 hours post-transfection.

PHM1-41 and UtSMC cells were trypsinized and washed with PBS (137 mM NaCl, 27 mM KCl, 100 mM Na_2HPO_4, 2 mM K_2HPO_4, pH 7.4). Electroporation was performed using the Basic Smooth Muscle Cell kit (Amaxa Inc., Gaithersburg, MD). 2×10^6 cells were pelleted and resuspended in 100 μl Basic Nucleofector solution together with 2 μg psiTC4 reporter, 1.5 μg pSH-TC4sh1-4 and 0.5 μg maxGFP vectors and transferred to the provided 2 mm cuvette. Cells were electroporated for 140 V, 35 ms in the time constant mode, using the Gene Pulser Xcell system (Bio-Rad, Hercules, CA), and were immediately diluted into 500 μl of pre-warmed culture media. Cells were dispensed (80 μl into 3 × 35-mm glass bottomed dishes for Ca^{2+} imaging experiments and 350 μl into a 100 mm dish for RNA analyses), and incubated for 24 h before media was replaced. Samples were analyzed 72-96 h after electroporation. A transfection efficiency of 60% was achieved.

2.5 mRNA isolation and quantitative real-time RT-PCR

Myometrial cell mRNA was isolated 72-96 h post-infection using the RNeasy kit (Qiagen, Valencia, CA). An on-column DNase digestion was performed using the RNase-free DNase set according to the manufacturer's instructions (Qiagen, Valencia, CA). Quantitative real-time PCR (RT-qPCR) was performed using 100 ng mRNA and the iScript one-step RT-PCR kit with SYBR Green (Bio-Rad, Hercules, CA) in an iCycler Thermal Cycler (Bio-Rad, Hercules,

CA). Previously designed PCR primers for TRPC1,3,5,6, and 7 [9] and newly designed primers for TRPC4, beta-glucuronidase (GUS), plasma membrane Ca^{2+}-ATPase isoform 1 (PMCA 1), PMCA 4, and sarcoplasmic endoplasmic reticulum Ca^{2+} ATPase isoform 2 (SERCA 2) (Table 1) were used at 500 nM. The PCR conditions were as follows: cDNA synthesis at 50°C for 30 min, iScript Reverse-transcriptase inactivation at 95°C for 5 min, PCR cycling where cDNA was denatured at 95°C for 15 sec, annealed at 60°C for 30 sec, and extended at 72°C for 1 min. Sequence integrity of RT-qPCR products was verified by direct sequencing. Melting curves for all products showed single peaks. Calculations were performed using the ΔΔCt method [22] where a given RNA was first normalized to GUS in each sample and then expressed relative to the corresponding value in cells infected with empty adenovirus.

RT-qPCR products for TRPCs and GUS, using 100 ng of RNA for TRPC1, TRPC4, TRPC6 and GUS and 1 μg of RNA for TRPC3, TRPC5 and TRPC7, were run in 3% agarose gels in 1× Tris-acetate-EDTA (TAE) electrophoresis buffer (40 mM Tris-acetate, 1mM EDTA, pH 8.0). Gels were then incubated in 1× TAE buffer with SYBR Green I nucleic acid gel stain (1:1000 dilution) for 30 min at room temperature with gentle rocking. Bands were visualized by using a Storm imager (Amersham Biosciences).

2.6 Immunoblotting

PHM1-41 cells (6×10^5) were plated in 100-mm dishes in culture medium and infected with adenovirus at an MOI of 1000. Cells were harvested after 72-96 h and whole cell extracts and plasma membrane extracts were prepared. For whole cell extract preparation, cells were lysed in modified RIPA buffer (50 mM Tris-HCl pH 7.4, 150 mM NaCl, 1% NP-40 (v/v), 1 mM EDTA, 0.25% Na-deoxycholate (v/v), 0.1% SDS (w/v)) plus protease inhibitor cocktail containing 1.04 mM 4-(2-Aminoethyl)benzenesulfonyl fluoride hydrochloride (AEBSF), 0.8 μM aprotinin, 21 μM leupeptin, 36 μM bestatin, 15 μM pepstatin A, 14 μM *trans*-Epoxysuccinyl-L-leucylamido(4-guanidino)butane (E-64). Lysates were incubated on ice for 10 min and sonicated on ice for 3 cycles at 10 sec/cycle, output setting 3, using a Micro Tip in a Branson Sonifier 250 (Danbury, CT). Mixtures were then centrifuged at 14,000 × g for 15 min at 4°C. The protein concentrations in the supernatants were measured by BCA Protein Assay (Pierce, Rockford, IL).

For plasma membrane preparation, a previously validated method [23] was adapted for use with small amounts of material. Cells were lysed in 200 μl homogenization buffer (100 mM KCl, 5 mM $MgCl_2$, 50 mM Tris-HCl, 1 mM EGTA, pH 7.2) plus protease inhibitor cocktail as above and sonicated on ice. Mixtures were centrifuged at 10,000 × g for 15 min at 4°C, and the resulting supernatants were centrifuged at 100,000 × g for 1 h at 4°C in a TLA100.3 rotor. The resulting pellets were dissolved in 10% ice-cold sucrose in homogenization buffer and layered over a layer of 28% sucrose in homogenization buffer. Samples were centrifuged at 57,000 × g for 30 min at 4°C in a TLS55 swinging bucket rotor. The plasma membrane fractions at the 10-28% sucrose interface were withdrawn and centrifuged at 100,000 × g for 30 min at 4°C. The resulting pellets were resuspended in modified RIPA buffer and stored at -80°C. The protein concentration was determined by BCA protein assay (Pierce Biotechnology, Rockford, IL).

Cell and membrane extracts were subjected to sodium dodecylsulfate-polyacrylamide electrophoresis in 8% gels and transferred to Millipore Immobilon-P transfer membrane (Billerica, MA). Immunoblots were probed with primary antibodies against TRPC1 (1:500) and TRPC4 (1:200). Primary polyclonal human PLCB3 (loading control) antibody and HRP-conjugated secondary antibodies were used at 1:2000 dilution. Where indicated, antibodies against TRPC4 and TRPC1 were preabsorbed prior to use with the corresponding antigenic peptides overnight at 4°C at mass ratios of 1:1 and 25:1 antigenic peptide:antibody, respectively, as recommended by the manufacturers. Bands were visualized by enhanced

chemiluminescence (ECL) reagent (Amersham Biosciences, GE Healthcare, Pittsburgh, PA). ECL signals were detected using a Storm imager and quantitation was accomplished by ImageQuant TL software (Amersham Biosciences).

2.7 Measurement of Intracellular Calcium

PHM1-41 and UtSMC cells were plated at 1×10^5 and 0.4×10^5 cells/ 0.8 ml, respectively, in 35-mm glass-bottomed dishes. Cells were loaded 72-96 h after infection at room temperature for 30 min with 5 μM Fura-2-AM and 0.1% Pluronic F-127 in fluorescence buffer (145 mM NaCl, 5 mM KCl, 1 mM Na_2HPO_4, 0.5 mM $MgCl_2$, 1 mM $CaCl_2$, 10 mM HEPES, 5 mM glucose, pH 7.4). Cells were then washed twice in the same buffer and incubated an additional 45 min at room temperature to allow for Fura-2 ester hydrolysis. Immediately prior to assay, cells were placed in Ca^{2+}-free fluorescence buffer (buffer containing 100 μM EGTA but no $CaCl_2$) and changes in fluorescence were measured at 340 and 380 nm excitation and 510 nm emission wavelengths in an ImCyt2 imaging system (Intracellular Imaging, Inc., Cincinnati, OH). Cells co-expressing eGFP were identified using an eGFP/fluorescein excitation filter (485 nm). Electroporated or virally infected cells did not display nonspecific membrane leaks, as evidenced by the fact that no significant increases in $[Ca^{2+}]_i$ were observed following addition of 1 mM $CaCl_2$ if cells were not exposed to stimuli eliciting SRCE. Changes in Ca^{2+} were observed in 20-45 cells/dish.

2.8 Electrophysiological Recordings

PHM1-41 cells exposed to adenoviral constructs expressing empty vector or TC4sh1 sequences were cultured on glass coverslips for >72 h prior to patch clamp experiments. Cultured cells were placed into a recording chamber (SA-OLY, Warner Instruments) at room temperature. Cell-attached recordings were performed using an AxoPatch 200B amplifier equipped with an Axon CV 203BU headstage (Axon Instruments). Recording electrodes (resistance, 3−5 MΩ) were pulled, polished, and coated with wax to reduce capacitance. Currents were filtered at 1 kHz, digitized at 40 kHz, and stored for subsequent analysis. Clampex and Clampfit versions 10.2 (Axon Instruments) were used for data acquisition and analysis, respectively. Pipette potential was clamped at -40 mV and all recordings were performed at room temperature (22° C). The bath solution was 125.4 mM NaCl, 20 mM tetraethylammounium chloride (TEA), 0.1 mM $MgCl_2$ 5 mM HEPES, 11 mM glucose, 1 μM $CaCl_2$, and 100 nM nifedipine. The pipette solution contained 135 mM CsCl, 2.5 mM $MgCl_2$, 10 mM HEPES, 10 mM glucose, 10 mM EGTA, and 10 μM paxilline (pH7.2). Cell-attached channel activity was recorded before and after addition of oxytocin (100 nM).

2.9 Data Analyses

Data are presented as mean ± S.E.M. and were analyzed by t-test or one-way ANOVA and Tukey's test, as appropriate, using Prism software (GraphPad Software, La Jolla CA) software. Changes in intracellular Ca^{2+} were analyzed using numerical analyses software (CalciumComp) developed by an engineer consultant (K. J. Bois, Fort Collins, CO). CalciumComp aligns the initial $[Ca^{2+}]_i$ peaks, removes noise, and calculates the extent of the increase $[Ca^{2+}]_i$ (peak height) and integrated area under the $[Ca^{2+}]_i$ transient curve. Data obtained using this method agreed within 95% with that analyzed by manual methods.

3. Results

3.1 A functional RNA interference mechanism is present in human myometrial cells

In order to study the function of endogenous TRPC4 in human myometrial cells, we designed 4 putative shRNA sequences that included a pre-microRNA backbone and tested them for their efficiency to decrease TRPC4 mRNA using the psiCHECK-2 system with a Renilla luciferase-

TRPC4 fusion reporter vector (psiTC4). The sequences of these constructs are listed in Table 1. Figure 1A shows that the four TRPC4-shRNA (TC4sh1-4) constructs produced between 68 and 94% reduction in Renilla luciferase protein expression compared to empty vector, a pUC19 vector, and a construct expressing a scrambled TRPC4 shRNA sequence (shx1).

RNAi requires expression and function of many components necessary for the production and processing of the shRNA constructs. To determine the effectiveness of this mechanism in processing the TC4sh1 construct in myometrial cells, the psiCHECK-2 TRPC4 reporter vector was electroporated into PHM1-41 and UtSMC cells, along with a plasmid expressing the TC4sh1 construct. Electroporation efficiency was ~60% as determined by visual assessment of maxGFP expression from a separate plasmid. TRPC4 mRNA was effectively targeted by the TC4sh1 construct, achieving >70 and 90% reduction of the reporter in PHM1-41 and UtSMC cells, respectively (Fig. 1B). These data indicated that the RNAi mechanism was adequate in myometrial cells and that the TC4sh1 targeting sequence was effective.

3.2 TRPC4 knockdown in human myometrial cells is TRPC4-specific and attenuates oxytocin- stimulated increases in $[Ca^{2+}]_i$

The TC4sh1 construct was cloned downstream of a U6 promoter into an adenoviral vector expressing GFP under the control of a separate CMV promoter. In PHM1-41 cells infected with the adenovirus expressing TC4sh1, significant TRPC4 mRNA knockdown occurred 48-96 h post infection, with the greatest knockdown at 72-96 h (data not shown). Fig. 2A shows that PHM1-41 cells infected with empty adenovirus displayed no changes in expression of any TRPC mRNA compared to noninfected cells. This demonstrates that viral infection itself did not alter TRPC expression. TRPC RT-qPCR amplicons show single products in agarose gels (Fig. 2B). In all cases, no product was observed if the reverse transcriptase was omitted from the mixture, indicating that there was no significant amplification of DNA in these samples. The adenoviral construct expressing TC4sh1 produced specific knockdown in TRPC4 mRNA, with no effect on other TRPC mRNAs 72 h post infection (real time RT-qPCR data are shown as supplementary data, Fig 1). Under these conditions, there were also no significant changes in the mRNAs for PMCA 1, PMCA 4 or SERCA 2 (supplementary data, Fig 2). The degree of TRPC4 knockdown was variable between experiments; we achieved a maximal knockdown of 73%, with a mean of 54 ± 3.28%. Fig. 3A and 3B show that TC4sh1 suppressed TRPC4 protein expression in both whole cell and purified plasma membrane extracts (by 40 % and 70% relative to empty vector, respectively). In contrast, the concentration of TRPC1 protein, the membrane expression of which has been reported to be enhanced by TRPC4 [5,24], was not significantly changed, relative to empty vector, in purified plasma membrane extracts.

The specificities of the TRPC4 and TRPC1 antibodies, as demonstrated by reduction in TRPC signal once the antibody was exposed to antigenic peptide, are shown in Fig 3C and Fig 3D, respectively. TRPC4 exhibited a band between 86 and 94 kDa in PHM1 cells using the TRPC4 antibody obtained from Alomone (and other suppliers). When transiently expressed in COSM6 cells, the TRPC4 overexpression (TRPC4 OE) vector produced a 100 kDa band detected with the HA tag that was reduced >70% when coexpressed with the TC4sh1 construct (Figure 3E). Differences in apparent size may represent differences in protein glycosylation in different cell types. Regardless, the suppression of expression of the HA-tagged protein by TC4sh1 further attests to its efficacy.

To assess effects of TRPC4 knockdown on increases in myometrial $[Ca^{2+}]_i$ in response to various stimuli, PHM1-41 cells were infected with adenoviral vectors carrying either empty vector or the TC4sh1 construct and tested for effects on SRCE, defined as a stimulus- and extracellular Ca^{2+}-dependent increase in $[Ca^{2+}]_i$. Noninfected PHM1-41 cells and cells infected with empty adenovirus behaved similarly with respect to the SRCE responses tested, indicating that viral infection per se had no effect on responsiveness (supplementary data, Fig.

3). The SRCE response is illustrated in the tracing in Fig. 4A (left panel). Cells were stimulated in Ca^{2+}-free buffer with oxytocin, a GPCR-activator resulting in IP_3 generation, eliciting a transient increase in $[Ca^{2+}]_i$. Once $[Ca^{2+}]_i$ returned to basal levels, 1 mM extracellular Ca^{2+} was added and SRCE was observed, as indicated by a second, extracellular Ca^{2+}-dependent increase in $[Ca^{2+}]_i$. No such increase was observed if the cells were not exposed to 1 mM extracellular Ca^{2+} or if Ca^{2+}-free buffer were added instead (data not shown). TRPC4 knockdown did not significantly affect the initial $[Ca^{2+}]_i$ transient but resulted in >70% inhibition of oxytocin-stimulated SRCE (dotted line in the tracing in Fig. 4A). In this particular experiment, a 73% reduction in TRPC4 mRNA knockdown was achieved (Fig. 4A, middle panel). The summarized data for individual cells are presented in the right panel of Fig. 4A.

Both the degree of TRPC4 mRNA knockdown and the extent of the inhibition of the oxytocin SRCE response were variable between experiments for reasons that we have yet to ascertain. Fig. 4B summarizes the effect of TRPC4 on inhibition of oxytocin-stimulated SRCE in 9 experiments (mean inhibition of 52 ± 3.61%). Importantly, the degree of inhibition of the oxytocin SRCE response correlated with the degree of TRPC4 knockdown (Fig. 4C) and the qualitative specificity of the response was always observed, regardless of the degree of knockdown. Furthermore, although considerably less efficient, we also used electroporation to introduce shRNA plasmids into PHM1-41 cells and observed a >45% decrease in TRPC4 mRNA and a >50% decrease in oxytocin-stimulated SRCE relative to empty vector in cells co-expressing GFP from a second plasmid (supplementary data, Fig. 4).

PHM1-41 cells are immortalized myometrial cells. Effects of oxytocin-stimulated increases in $[Ca^{2+}]_i$ were also observed in UtSMC cells. Fig. 5 shows >77% and >65% inhibition of the $[Ca^{2+}]_i$ transient area and peak height, respectively, of the oxytocin-stimulated SRCE response in an experiment where > 67% mRNA knockdown was achieved.

3.3 TRPC4 knockdown attenuates SRCE stimulated by other G protein-coupled receptors

In order to determine if the effect of TRPC4 knockdown was specific to oxytocin signaling or pertained to other GPCR stimulants, we examined the effect of TRPC4 knockdown on SRCE elicited in response to stimulation of PHM1-41 cells with ATP and PGF2α. Significant suppression of SRCE induced by ATP (65% and 79% inhibition of area and peak height, respectively) and PGF2α (86% and 79% inhibition of area and peak height, respectively) was observed in cells infected with adenovirus expressing TC4sh1, but not with empty vector (Fig. 6). In unrelated studies, we have determined that ATP effects on phospholipase C beta activation in PHM1-41 cells are inhibited by Reactive Blue-2, a P2Y-specific inhibitor, indicating that the action of ATP is GPCR-mediated (D. Murtazina, unpublished observations). These data support a link between TRPC4 knockdown and attenuation of GPCR-stimulated calcium entry in myometrial cells.

3.4 TRPC4 knockdown had no effect on thapsigargin- or diacylglycerol-stimulated extracellular calcium-dependent increases in $[Ca^{2+}]_i$ in human myometrial cells

Using the same experimental design as in Fig. 4, the effect of TRPC4 knockdown on store-operated SRCE elicited by exposure to thapsigargin, which induces Ca^{2+} store depletion by blocking the endoplasmic reticulum Ca^{2+}-ATPase, was determined. Thapsigargin (TG) treatment resulted in an increase in $[Ca^{2+}]_i$ in the absence of extracellular Ca^{2+} (Fig. 7A) Notably, in contrast to the effect of TRPC4 knockdown on oxytocin-stimulated SRCE, the thapsigargin-stimulated SRCE observed in response to the addition of extracellular Ca^{2+} was not affected by TRPC4 knockdown. Similarly, no significant changes were observed in the elevation of $[Ca^{2+}]_i$ elicited in the presence of extracellular $Ca^{2+}$by OAG, a cell permeable diacylglycerol (Fig 7B). In UtSMC, knockdown of TRPC4 also did not alter the thapsigargin response (supplementary data, Fig. 5).

3.5 Activation of cation currents by oxytocin in PHM1-41 cells was attenuated by the expression of TC4sh1

Using cell-attached patch clamp electrophysiology, single channel activity was recorded in response to 100 nM oxytocin in PHM1-41 cells. In these experiments, potential contributions from L-type calcium channels were minimized by inclusion of 100 nM nifedipine in the bath solution. Furthermore, a significant contribution to OT-stimulated currents from BK_{Ca} channels activated by calcium entry, as previously reported [25], were essentially eliminated by inclusion of 20 mM TEA in the bath solution and 10 μM paxilline in the pipette solution. Fig. 8A shows a representative baseline recording with distinct single channel openings (Control). The administration of oxytocin increased both the frequency and duration of channel activity in cells infected with empty control vector (Fig 8A, Control + OT). Cells in which TRPC4 expression was suppressed by TC4sh1 showed significantly lower response to oxytocin (Fig 8B, TC4sh1 + OT). The change in total open probability (ΔNP_o) in response to oxytocin was significantly reduced in cells treated with TC4sh1 versus cells treated with empty vector (Fig. 8C).

4. Discussion

TRPC proteins have been implicated in calcium signaling dynamics in myometrial smooth muscle [6,12,26]. Previous studies have shown that, although human myometrium expresses most TPRC mRNAs, TRPC4 and TRPC1 mRNAs are expressed in high relative abundance, along with TRPC6 [9]. However, to date, no TRPC knockdown studies have been conducted in this system. Since the TRPC profile can be dramatically different between systems and since profile is hypothesized to dictate the physiological function of the homo- and heterotetrameric TRPC channels that are formed, it is important to determine the role of specific TRPC proteins in affecting signal-stimulated myometrial calcium dynamics.

Most TRPC4 studies have focused on the functional properties of exogenously overexpressed TRPC4 channels. Some studies indicate that TRPC4, and the closely related TRPC5 channels, are receptor-operated cation channels activated in a phospholipase C-dependent manner. Other studies define these channels as Ca^{2+}-permeable, nonselective cation channels, activated independent of IP_3-R activation or Ca^{2+}-store depletion, whereas still others suggest activation by store depletion, with or without a potential interaction with TRPC1 [27-29]. Members of the TRPC3/6/7 subfamily can associate with each other into homo- and heterotetramers, as can members of the TRPC1/4/5 subfamily. Some reports indicate that neither group can associate with members of the other group [30-32], but others indicate association between members of both groups [33,34]. Because of the putative heterotetrameric nature of the TRPC channels, overexpression may not replicate the endogenous configuration of channels containing TRPC4 in a particular tissue and may promote interactions with other proteins that do not normally occur when TRPC4 is present at endogenous concentrations. Hence, these studies show that channels containing TRPC4 are capable of responding to a wide variety of stimuli, but do not rule out greater specificity in a physiological context.

In an attempt to assess the role of endogenous TRPC4 in myometrial SRCE in response to various stimuli, we used RNA interference to diminish its expression. Since PHM1-41 and UtSMC cells are difficult to transfect by conventional methods (<40% efficiency) and are not easily selectable, we used a viral vector to express the shRNA constructs. Despite demonstrating that the shRNA construct was effective at targeting an exogenous TRPC4 reporter for degradation, we experienced a variable degree of endogenous TRPC4 knockdown using an adenoviral vector between experiments. Although adenoviral vectors usually achieve 90-95% infection efficiency with minimal cell toxicity, variability in the efficiency of knockdowns using viral shRNA constructs has been reported [35,36]. Additionally, smooth muscle cells display low adenovirus binding levels, potentially due either to the lack or low

expression of Coxsackie Adenovirus Receptor (CAR) [37], which could contribute to variability.

The data indicate that TRPC4 mRNA and protein expression were specifically diminished in PHM1-41 and UtSMC by the adenoviral construct expressing TC4sh1, while concentrations of other TRPCs were unaffected. PHM1-41 and UtSMC cells, as well as rat myometrial cells, respond to oxytocin with increases in $[Ca^{2+}]_i$ that are partially dependent on extracellular Ca^{2+} and are not affected by voltage-operated channels (VOC) blockers such as nifedipine [12,16,17]. Reduction in TRPC4 expression preferentially attenuated GPCR-operated SRCE in PHM1-41 and UtSMC cells. This appears to be a relatively general mechanism, as oxytocin, PGF2α and ATP-mediated SRCE were also affected. Both oxytocin and PGF2α are important endogenous stimulators of uterine contractions and play important roles during labor [38]. In contrast, TRPC4 knockdown did not affect thapsigargin- or OAG-stimulated SRCE. The finding that suppression of a single endogenous TRPC in myometrial cells affected a specific type of SRCE response is further supported by our recent observation that suppression of expression of TRPC6 has very different effects (YS Kim, A. Ulloa, D. Chung and B. Sanborn, manuscript in preparation).

We also observed an increase in ion channel activity after oxytocin stimulation in cell-attached patches on cells infected with empty adenoviral vector. This activity was observed in the presence of nifedipine, paxilline and TEA, suggesting that it was not due to nifedipine-sensitive L-type channels or BK_{Ca} channels. Importantly, oxytocin-stimulated channel activity was markedly inhibited by expression of TC4sh1. This observation adds further support to the contention that TRPC4 plays an important role in oxytocin-mediated SRCE.

The effects of endogenous TRPC4 knockdown in myometrial cells are similar in some respects but not others to effects noted in other studies. TRPC4 antisense as well as TRPC4 siRNA constructs inhibited both GPCR- and OAG-stimulated but not thapsigargin-stimulated Sr^{2+} or Ba^{2+} entry in HEK cells expressing endogenous TRPCs [39,40]. In contrast, no effect of TRPC4 knockdown on methacholine-mediated increases in $[Ca^{2+}]_i$ in HEK293 cells was noted [41]. HEK cells have a very different TRPC profile than myometrial cells, and endogenous channel composition may be quite different. The specific effect of TRPC4 knockdown on GPCR-stimulated SRCE suggests that tetrameric channels in myometrial cells that contain a significant proportion of TRPC4 may be affected by activation of the GPCRs tested, either as a result of direct interactions, signalplex organization or possibly as a result of co-localization in membrane subdomains. TRPC channels can assemble into signaling complexes containing proteins such as caveolin-1, $G_{\alpha q/11}$ and PLCB3 [32]. TRPC4 and TRPC5 also contain multiple binding motifs and domains (CaM, CIRB, protein 4.1-, PDZ, and auto-inhibitory) that may contribute to interaction with other proteins as well as to regulation of activity [28].

In the myometrium, both TRPC4 and TRPC1 are expressed, increasing the possibility that some endogenous TRPC heterotetramers include these two proteins. Although there are reports of GPCR-linked Ca^{2+} entry and currents in cells overexpressing TRPC1, this protein has been linked most often to thapsigargin-stimulated SRCE and store-operated electrical activity [3]. The most obvious interpretation for our data is that endogenous TRPC4 is primarily responsible for GPCR-stimulated SRCE response in myometrial cells. Alternatively, TRPC4 has been reported to enhance the localization of TRPC1 in the plasma membrane [5,24]. However, since no changes in plasma membrane expression of TRPC1 in response to a TRPC4 knockdown were detected, it is unlikely that TRPC4 knockdown disrupts GPCR-mediated SRCE indirectly by reducing TPRC1 concentration at the cell surface in myometrium. While we cannot totally rule out contributions by other TRPC channels expressed at significantly lower mRNA levels, it seems less likely that these TRPCs would significantly contribute to formation of heterotetrameric channels involved in the TRPC4-sensitive parameters measured here.

Although TRPC4 knockdown did not affect PMCA or SERCA pump mRNA, the possibility that changes in expression or activity of these proteins may affect the dynamics of the $[Ca^{2+}]_i$ transients cannot be excluded.

The activation of the SRCE response by GPCRs in myometrial cells appears to be largely dependent on phospholipase C activation [11,12]. Capacitative or receptor- and store-operated Ca^{2+} entry have been postulated to involve IP_3-R activation, conformation coupling mechanisms, or signals generated by release of Ca^{2+} from intracellular stores [4]. Alternatively, phosphatidylinositol bisphosphate (PIP_2) may exert an inhibitory effect on TRPC4 and TRPC5 which is relieved by the GPCR-mediated degradation of PIP_2 by phospholipase C, resulting in channel activation [42]. STIM1 and Orai1, predominantly endoplasmic reticulum and plasma membrane proteins, respectively, have been implicated in the Ca^{2+} entry response to endoplasmic reticulum store depletion resulting from Ca^{2+}-ATPase inhibition [33,43]. Stimulation of SRCE or Ca^{2+} currents by some, but not all, GPCRs has been reported to be attenuated by STIM1 knockdown or by STIM1 dominant negative expression [33,41]. Overexpression studies indicate that TRPC1, 4, and 5 can physically interact with STIM1 whereas TRPC3, 6, and 7 do not do so [44,45]. Other studies implicate Orai1 as a binding partner of TRPC3 and TRPC6 channels [46]. In this case, the STIM/Orai interaction stimulated by decreases in Ca^{2+} stores has been postulated to decrease the Orai/TPRC interaction and promote TPRC activation. The involvement of STIM or Orai in GPCR-stimulated SRCE in myometrium remains to be explored, but the lack of an effect of TRPC4 knockdown on thapsigargin-stimulated SRCE suggests that any potential TRPC4/STIM1 interaction would not contribute markedly to this effect.

Evidence for a separate Ca^{2+} entry pathway involving intracellular phospholipase A2 activation by a calcium influx factor (CIF) generated in response to release of Ca^{2+} from intracellular stores has been reported [47]. Although the current studies do not directly address this pathway, the lack of effect of TRPC4 knockdown on thapsigargin-mediated SRCE suggests that this mechanism is not a major component of the GPCR response in myometrial cells.

Studies in TRPC4 -/- mice implicate TRPC4 in agonist-induced Ca^{2+} entry [48]. Ca^{2+} entry induced by thrombin was significantly diminished in aortic and lung vascular endothelial cells isolated from TRPC4 -/- mice, leading to impaired regulation of vascular tone and permeability. Interestingly, the TPRC6 mRNA PCR product [49] appears to be more intense in TRPC4 -/- compared to wild-type mice. Primary aorta endothelial cells isolated from TRPC4 -/- mice exhibited diminished Ca^{2+} entry stimulated by SERCA inhibition [48].

In the present study, OAG-mediated SRCE, which we have previously shown to be protein kinase C-independent [13], was not significantly affected by TRPC4 knockdown. In contrast, TRPC4 knockdown attenuated OAG-stimulated Ba^{2+} entry in HEK-293 cells [40]. Other studies have shown a negative regulatory effect of diacylglycerol on overexpressed TRPC4 and TRPC5 activation mediated by protein kinase C in DT40 B-cells [50]. In myometrial cells, TRPC4 may not be a major contributor to the overall OAG response in myometrial cells if OAG exerts an inhibitory effect. GPCR-mediated SRCE was never completely inhibited by TRPC4 knockdown, however, leaving open the possibility that a portion of the SRCE response to GPCRs might involve activation of other TRPCs as a result of localized GPCR-stimulated diacylglycerol production.

In response to stretch, human pregnant myometrial cells exhibit an increase in TRPC3 and TRPC4 mRNA, TRPC3 protein expression, and cyclopiazonic acid-induced store depletion [26]. Interleukin-1β specifically upregulated TRPC3 protein expression in myometrial cells without influencing TRPC3 mRNA and had no effect of TRPC4 mRNA or protein [8].

Significant increases in myometrial TRPC6 and TRPC7 mRNAs and TRPC3, TRPC4 and TRPC6 proteins have been reported in human myometrial term at labor compared to term not in labor samples [8]. In another study, a specific decrease in TRPC4 mRNA, but not protein was observed with the onset of labor in human fundal myometrium, with no changes in TRPC1, TRPC3 and TRPC6 mRNA or protein [9]. The basis for the discrepancies between these studies and for the lack of correlation between changes in TRPC mRNA and protein are still unknown.

The data presented here support our hypothesis that specific signals can affect specific types of signal-regulated Ca^{2+} entry in the myometrium. This work increases our understanding of the regulation of Ca^{2+} dynamics in myometrial cells and points to a specific role for TRPC4 in GPCR-regulated myometrial Ca^{2+} dynamics. The data suggest that this contribution, in addition to the important role in Ca^{2+} homeostasis played by voltage-operated channels and the influences of Ca^{2+} pumps, exchangers and potassium channels, provide the myometrium with the ability to respond in specific and precise ways to influences in its environment, both during pregnancy and at the time of parturition.

Supplementary Material

Refer to Web version on PubMed Central for supplementary material.

Acknowledgments

We thank G. Hannon for the pSHAG vector, J.W. Putney Jr. for the TRPC4 cDNA clone and K.J. Bois for creating CalciumComp. This work was supported in part by NIHF31-HD051037 (AU), NIHT32-HD0703, NIH HD38970 and March of Dimes #6-FY05-77 (BMS), AHA 0535226N (SE), and NIHF31-HL09414 (ALG). This work was completed in partial fulfillment of the requirement of the Ph.D. degree by A.U.

References

1. Word RA, Tang DC, Kamm KE. Activation properties of myosin light chain kinase during contraction/relaxation cycles of tonic and phasic smooth muscles. J Biol Chem 1994;269:21596–21602. [PubMed: 8063799]
2. Ramsey IS, Delling M, Clapham DE. An introduction to TRP channels. Annu Rev Physiol 2006;68:619–647. [PubMed: 16460286]
3. Parekh AB, Putney JW Jr. Store-operated calcium channels. Physiol Rev 2005;85:757–810. [PubMed: 15788710]
4. Putney JW Jr. Recent breakthroughs in the molecular mechanism of capacitative calcium entry (with thoughts on how we got here). Cell Calcium 2007;42:103–110. [PubMed: 17349691]
5. Hofmann T, Schaefer M, Schultz G, Gudermann T. Subunit composition of mammalian transient receptor potential channels in living cells. Proc Natl Acad Sci U S A 2002;99:7461–7466. [PubMed: 12032305]
6. Yang M, Gupta A, Shlykov SG, Corrigan R, Tsujimoto S, Sanborn BM. Multiple Trp isoforms implicated in capacitative calcium entry are expressed in human pregnant myometrium and myometrial cells. Biol Reprod 2002;67:988–994. [PubMed: 12193412]
7. Dalrymple A, Slater DM, Beech D, Poston L, Tribe RM. Molecular identification and localization of Trp homologues, putative calcium channels, in pregnant human uterus. Mol Hum Reprod 2002;8:946–951. [PubMed: 12356946]
8. Dalrymple A, Slater DM, Poston L, Tribe RM. Physiological induction of transient receptor potential canonical proteins, calcium entry channels, in human myometrium: influence of pregnancy, labor, and interleukin-1 beta. J Clin Endocrinol Metab 2004;89:1291–1300. [PubMed: 15001625]
9. Ku CY, Babich L, Word RA, et al. Expression of transient receptor channel proteins in human fundal myometrium in pregnancy. J Soc Gynecol Investig 2006;13:217–225.
10. Monga M, Ku CY, Dodge K, Sanborn BM. Oxytocin-stimulated responses in a pregnant human immortalized myometrial cell line. Biol Reprod 1996;55:427–432. [PubMed: 8828850]

11. Monga M, Campbell DF, Sanborn BM. Oxytocin-stimulated capacitative calcium entry in human myometrial cells. Am J Obstet Gynecol 1999;181:424–429. [PubMed: 10454695]
12. Shlykov SG, Yang M, Alcorn JL, Sanborn BM. Capacitative cation entry in human myometrial cells and augmentation by hTrpC3 overexpression. Biol Reprod 2003;69:647–655. [PubMed: 12700192]
13. Shlykov SG, Sanborn BM. Stimulation of intracellular Ca2+ oscillations by diacylglycerol in human myometrial cells. Cell Calcium 2004;36:157–164. [PubMed: 15193863]
14. Wray S, Jones K, Kupittayanant S, et al. Calcium signaling and uterine contractility. J Soc Gynecol Investig 2003;10:252–264.
15. Sanborn BM. Hormonal signaling and signal pathway crosstalk in the control of myometrial calcium dynamics. Semin Cell Dev Biol 2007;18:305–314. [PubMed: 17627855]
16. Anwer K, Sanborn BM. Changes in intracellular free calcium in isolated myometrial cells: role of extracellular and intracellular calcium and possible involvement of guanine nucleotide-sensitive proteins. Endocrinology 1989;124:17–23. [PubMed: 2491804]
17. Burghardt RC, Barhoumi R, Sanborn BM, Andersen J. Oxytocin-induced Ca2+ responses in human myometrial cells. Biol Reprod 1999;60:777–782. [PubMed: 10084948]
18. Pollard AJ, Krainer AR, Robson SC, Europe-Finner GN. Alternative splicing of the adenylyl cyclase stimulatory G-protein G alpha(s) is regulated by SF2/ASF and heterogeneous nuclear ribonucleoprotein A1 (hnRNPA1) and involves the use of an unusual TG 3′-splice Site. J Biol Chem 2002;277:15241–15251. [PubMed: 11825891]
19. Ciarmela P, Wiater E, Vale W. Activin-A in myometrium: characterization of the actions on myometrial cells. Endocrinology 2008;149:2506–2516. [PubMed: 18239071]
20. Reynolds A, Leake D, Boese Q, Scaringe S, Marshall WS, Khvorova A. Rational siRNA design for RNA interference. Nat Biotechnol 2004;22:326–330. [PubMed: 14758366]
21. Boden D, Pusch O, Silbermann R, Lee F, Tucker L, Ramratnam B. Enhanced gene silencing of HIV-1 specific siRNA using microRNA designed hairpins. Nucleic Acids Res 2004;32:1154–1158. [PubMed: 14966264]
22. Pfaffl MW. A new mathematical model for relative quantification in real-time RT-PCR. Nucleic Acids Res 2001;29:e45. [PubMed: 11328886]
23. Wen Y, Anwer K, Singh SP, Sanborn BM. Protein kinase-A inhibits phospholipase-C activity and alters protein phosphorylation in rat myometrial plasma membranes. Endocrinology 1992;131:1377–1382. [PubMed: 1324160]
24. Alfonso S, Benito O, Alicia S, et al. Regulation of the cellular localization and function of human transient receptor potential channel 1 by other members of the TRPC family. Cell Calcium 2008;43:375–387. [PubMed: 17850866]
25. L S, S F, K M, W T, Zhou XB. Oxytocin receptors differentially signal via Gq and Gi proteins in pregnant and nonpregnant rat uterine myocytes: implications for myometrial contractility. Molecular Endocrinology 2007;21:740–752. [PubMed: 17170070]
26. Dalrymple A, Mahn K, Poston L, Songu-Mize E, Tribe RM. Mechanical stretch regulates TRPC expression and calcium entry in human myometrial smooth muscle cells. Mol Hum Reprod 2007;13:171–179. [PubMed: 17208928]
27. Vanden AF, Lemonnier L, Thebault S, et al. Two types of store-operated Ca2+ channels with different activation modes and molecular origin in LNCaP human prostate cancer epithelial cells. J Biol Chem 2004;279:30326–30337. [PubMed: 15138280]
28. Plant TD, Schaefer M. Receptor-operated cation channels formed by TRPC4 and TRPC5. Naunyn Schmiedebergs Arch Pharmacol 2005;371:266–276. [PubMed: 15902430]
29. Abad E, Lorente G, Gavara N, Morales M, Gual A, Gasull X. Activation of store-operated Ca(2+) channels in trabecular meshwork cells. Invest Ophthalmol Vis Sci 2008;49:677–686. [PubMed: 18235014]
30. Amiri H, Schultz G, Schaefer M. FRET-based analysis of TRPC subunit stoichiometry. Cell Calcium 2003;33:463–470. [PubMed: 12765691]
31. Schilling WP, Goel M. Mammalian TRPC channel subunit assembly. Novartis Found Symp 2004;258:18–30. [PubMed: 15104174]

32. Ambudkar IS, Bandyopadhyay BC, Liu X, Lockwich TP, Paria B, Ong HL. Functional organization of TRPC-Ca2+ channels and regulation of calcium microdomains. Cell Calcium 2006;40:495–504. [PubMed: 17030060]
33. Yuan JP, Zeng W, Huang GN, Worley PF, Muallem S. STIM1 heteromultimerizes TRPC channels to determine their function as store-operated channels. Nat Cell Biol 2007;9:636–645. [PubMed: 17486119]
34. Saleh SN, Albert AP, Large WA. Diverse properties of store-operated TRPC channels activated by protein kinase C in vascular myocytes. J Physiol. 2008
35. Arts GJ, Langemeijer E, Tissingh R, et al. Adenoviral vectors expressing siRNAs for discovery and validation of gene function. Genome Res 2003;13:2325–2332. [PubMed: 12975310]
36. Jones RJ, Jourd'heuil D, Salerno JC, Smith SM, Singer HA. iNOS regulation by calcium/calmodulin-dependent protein kinase II in vascular smooth muscle. Am J Physiol Heart Circ Physiol 2007;292:H2634–H2642. [PubMed: 17293490]
37. Wickham TJ, Segal DM, Roelvink PW, et al. Targeted adenovirus gene transfer to endothelial and smooth muscle cells by using bispecific antibodies. J Virol 1996;70:6831–6838. [PubMed: 8794324]
38. Challis JRG, Matthews SG, Gibb W, Lye SJ. Endocrine and paracrine regulation of birth at term and preterm. Endocr Rev 2000;21:514–550. [PubMed: 11041447]
39. Wu X, Babnigg G, Zagranichnaya T, Villereal ML. The role of endogenous human Trp4 in regulating carbachol-induced calcium oscillations in HEK-293 cells. J Biol Chem 2002;277:13597–13608. [PubMed: 11830588]
40. Zagranichnaya TK, Wu X, M L. Villereal, Endogenous TRPC1, TRPC3, and TRPC7 proteins combine to form native store-operated channels in HEK-293 cells. J Biol Chem 2005;280:29559–29569. [PubMed: 15972814]
41. Wedel B, Boyles RR, Putney JW Jr, Bird GS. Role of the store-operated calcium entry proteins Stim1 and Orai1 in muscarinic cholinergic receptor-stimulated calcium oscillations in human embryonic kidney cells. J Physiol 2007;579:679–689. [PubMed: 17218358]
42. Putney JW Jr. Inositol lipids and TRPC channel activation. Biochem Soc Symp 2007:37–45. [PubMed: 17233578]
43. Smyth JT, Dehaven WI, Jones BF, et al. Emerging perspectives in store-operated Ca2+ entry: roles of Orai, Stim and TRP. Biochim Biophys Acta 2006;1763:1147–1160. [PubMed: 17034882]
44. Huang GN, Zeng W, Kim JY, et al. STIM1 carboxyl-terminus activates native SOC, I(crac) and TRPC1 channels. Nat Cell Biol 2006;8:1003–1010. [PubMed: 16906149]
45. Worley PF, Zeng W, Huang GN, et al. TRPC channels as STIM1-regulated store-operated channels. Cell Calcium 2007;42:205–211. [PubMed: 17517433]
46. Liao Y, Erxleben C, Yildirim E, Abramowitz J, Armstrong DL, Birnbaumer L. Orai proteins interact with TRPC channels and confer responsiveness to store depletion. Proc Natl Acad Sci U S A 2007;104:4682–4687. [PubMed: 17360584]
47. Bolotina VM, Csutora P. CIF and other mysteries of the store-operated Ca2+- entry pathway. Trends Biochem Sci 2005;30:378–387. [PubMed: 15951181]
48. Freichel M, Vennekens R, Olausson J, et al. Functional role of TRPC proteins in native systems: implications from knockout and knock-down studies. J Physiol 2005;567:59–66. [PubMed: 15975974]
49. Tiruppathi C, Freichel M, Vogel SM, et al. Impairment of store-operated Ca2+ entry in TRPC4(-/-) mice interferes with increase in lung microvascular permeability. Circ Res 2002;91:70–76. [PubMed: 12114324]
50. Venkatachalam K, Zheng F, Gill DL. Control of TRPC and store-operated channels by protein kinase C. Novartis Found Symp 2004;258:172–185. [PubMed: 15104182]

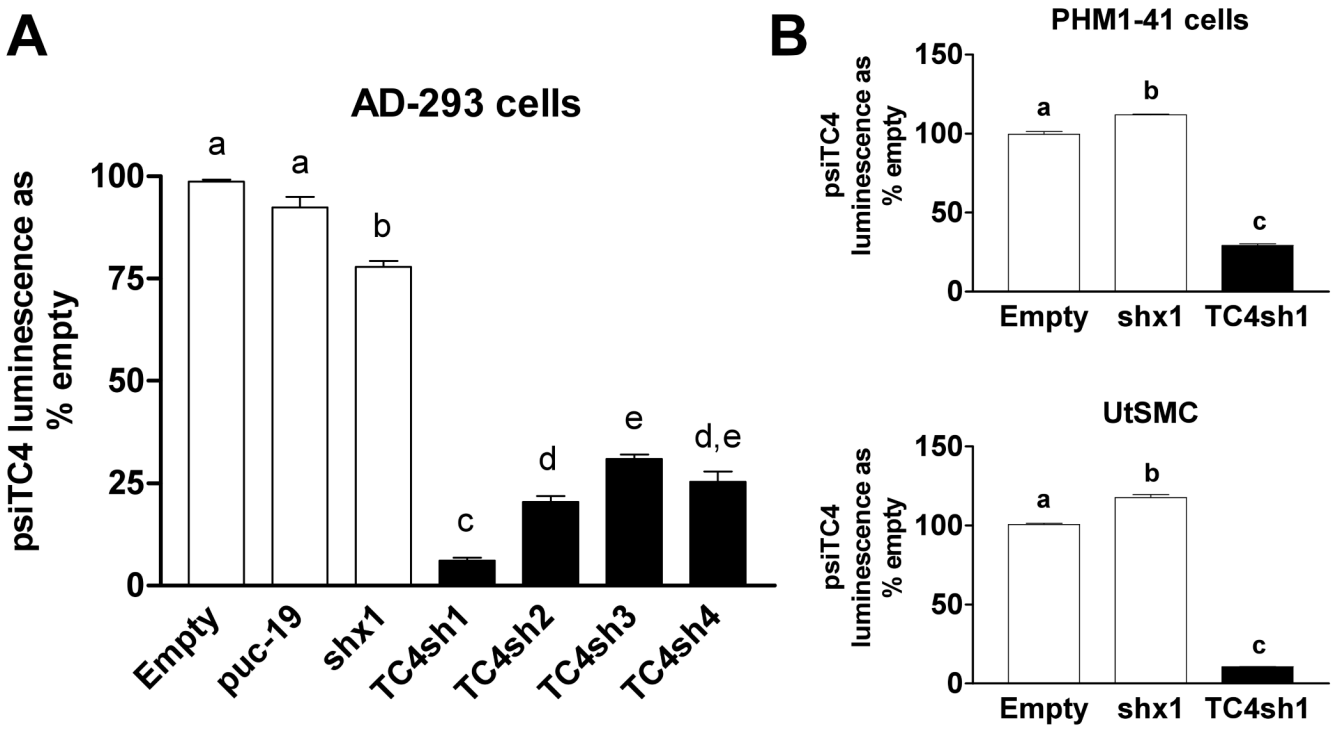

Fig. 1.

TRPC4-reporter mRNA is suppressed by TRPC4-shRNA constructs in AD-293, PHM1-41 and UtSMC cells. (A) Significant suppression of luminescence from a Renilla luciferase-TRPC4 fusion reporter (psiTC4) following co-transfection of the reporter and plasmids expressing TRPC4 shRNAs (TC4sh1-4) in AD-293 cells as described in Methods. Controls include empty vector, puc-19 vector and scrambled shRNA (shx1). (B) psiTC4 was electroporated into PHM1-41 and UtSMC cells, together with TRPC4-shRNA#1 (TC4sh1) in pSHAG vector as described in Methods. Controls include empty vector (pSHAG) and pSHAG plasmid expressing a scrambled shRNA control sequence (shx1). In A and B samples were isolated >72 h post-electroporation. Data are expressed as % of luminescence exhibited by co-transfection of empty vector and represent mean ± S.E.M. (n=3). Background luminescence (~7%) was subtracted from all samples. Data were analyzed by one-way ANOVA and Tukey's test. Significant difference between groups ($p<0.05$) is indicated by different lowercase letters.

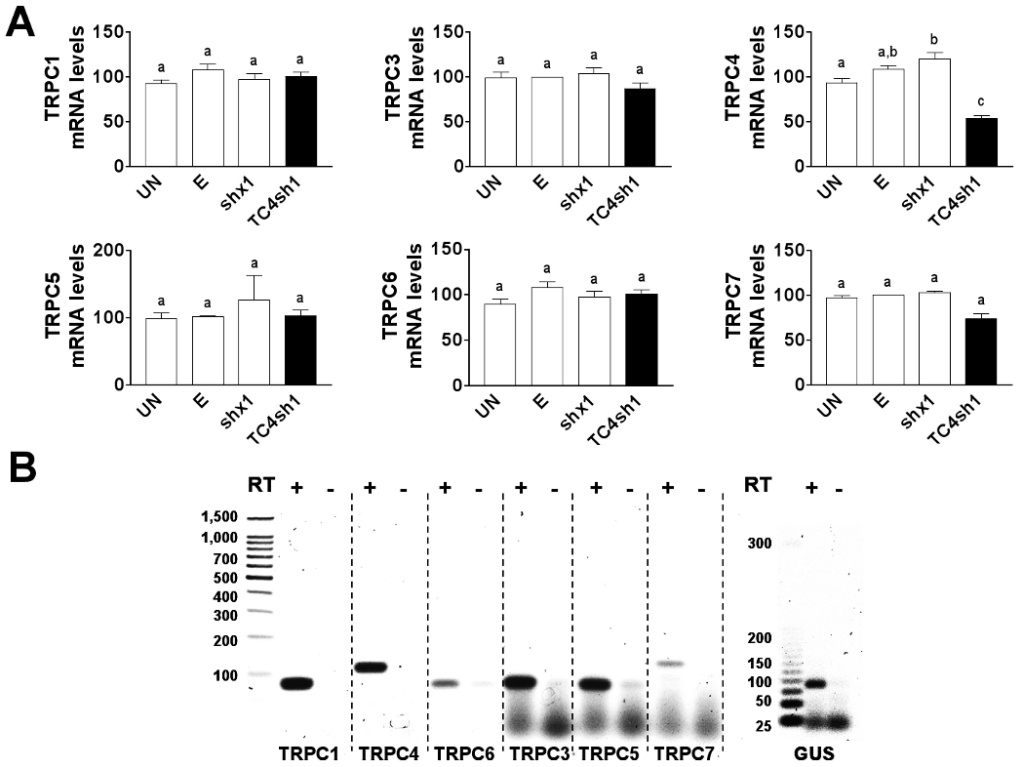

Fig. 2.

Adenovirus vector expressing TC4sh1 produced a specific TRPC4 mRNA knockdown in PHM1-41 cells. (A) PHM1-41 infection with adenovirus expressing TC4sh1 induced specific TRPC4 mRNA knockdown compared to effects of empty vector (E) or scrambled shRNA (shx1). Also shown are the TRPC mRNA levels in PHM1-41 cells not treated with adenovirus (UN). mRNA levels of other TRPCs are unchanged by exposure to any of these viral constructs. mRNA was normalized to GUS in the same sample and expressed relative to the value in cells exposed to empty vector. In all cases, data represent the mean ± S.E.M. (n=3); significant differences between groups ($p<0.05$), as analyzed by one-way ANOVA and Tukey's test, are indicated by different lowercase letters. (B) RT-qPCR products for TRPC1, TRPC4, TRPC6, and GUS (obtained from 100 ng RNA) as well as for TRPC3, TRPC5 and TRPC7 (obtained from 1 μg RNA) were run in 3% agarose gels. In all cases, single bands of the expected size were observed. No bands are observed in samples lacking reverse transcriptase (RT) in the reaction.

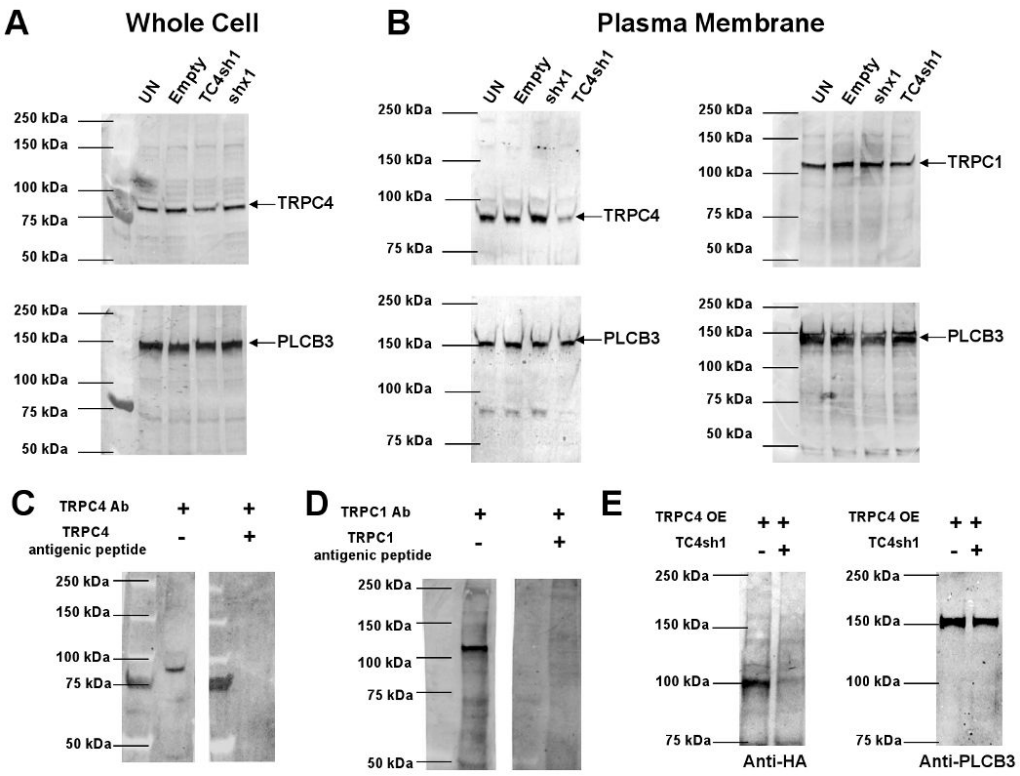

Fig 3.

Adenovirus vector expressing TC4sh1 produced a specific TRPC4 protein knockdown in PHM1-41 cells. (A). whole cell extracts and (B) purified membrane extracts from uninfected (UN) cells and cells exposed to empty adenovirus (E), virus expressing a scrambled shRNA sequence (shx1), or virus expressing TC4sh1 for > 72 h. PLCB3 was used as normalization control. (C) TRPC4 antibody (Ab) specificity is shown by the absence of 92 kDa band when the antibody was preabsorbed with TRPC4 antigenic peptide. (D) Antibody preabsorption usingTRPC1 antigenic peptide specifically blocks 116 KDa TRPC1 band detection by the TRPC1 antibody (Ab). (E) Expression of the TRPC4-HA tag protein overexpressed (TRPC4 OE) in COSM6 cells and suppression of this expression by cotransfection with the TC4sh1 construct.

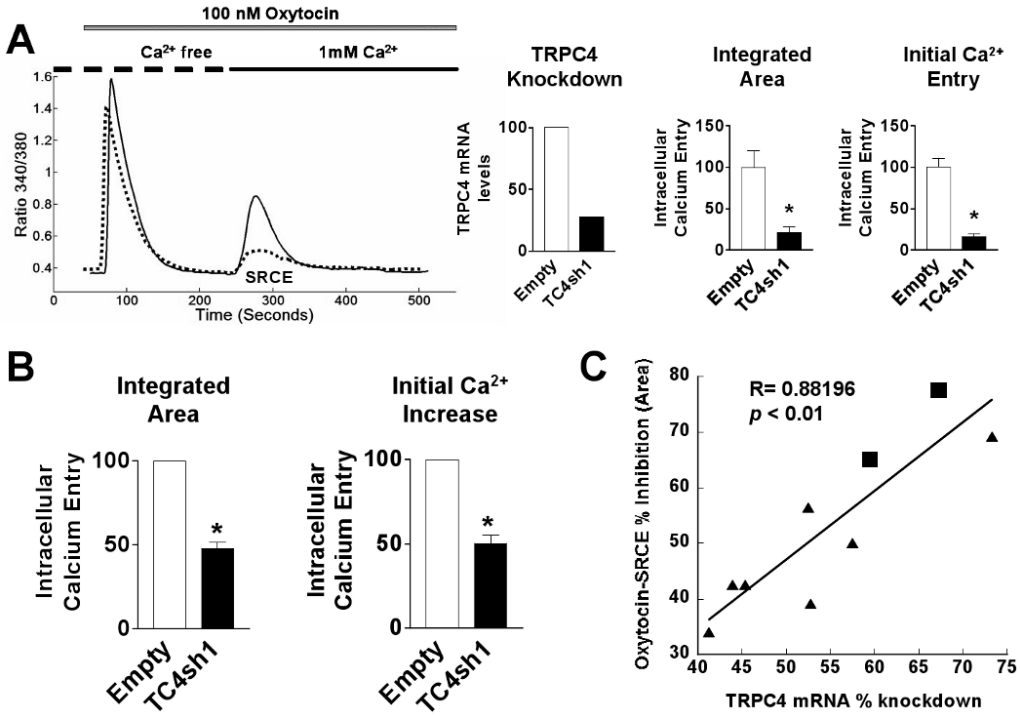

Fig 4.

Attenuation of oxytocin signal-regulated calcium entry (SRCE) induced by TRPC4 knockdown in PHM1-41 cells. (A) *Left*. SRCE induced by 100 nM oxytocin in PHM1-41 cells infected with either empty adenovirus (empty, solid line) or adenovirus expressing TC4sh1 (dotted line) for >72 h. *Middle*. TRPC4 mRNA levels, normalized relative to empty vector, in the experiment shown. *Right*. Mean ± S.E.M. (n= 20-40 cells) of changes in $[Ca^{2+}]i$ resulting from addition of 1 mM extracellular Ca^{2+} (SRCE) in the experiment shown, calculated as area under the curve (integrated area) and by peak height (initial calcium entry). (B) Mean changes in $[Ca^{2+}]i$ observed in 9 experiments. Data are presented as mean ± S.E.M. and were analyzed by t-test. In all cases, significant differences between groups ($p<0.05$) are indicated by an asterisk (*). (C) TRPC4 mRNA knockdown is strongly correlated with attenuation of the oxytocin-SRCE response (R= 0.88196, ρ = <0.01). Data samples are from PHM1-41 cells (circles) and UtSMC experiments (squares).

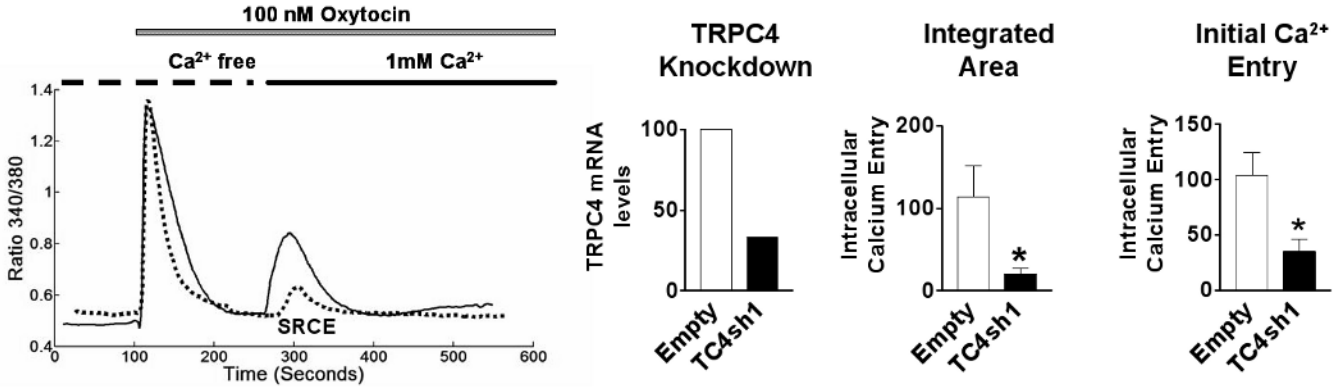

Fig. 5.

Specific TRPC4 mRNA knockdown and inhibition of oxytocin-stimulated SRCE in UtSMC cells. *Left*. SRCE induced by 100 nM oxytocin in UtSMC cells infected for >72 h with empty vector (empty, solid lines) or adenovirus expressing TC4sh1 (dotted line). *Middle*. TRPC4 mRNA, normalized relative to empty vector, in the experiment shown .*Right*. Mean changes in $[Ca^{2+}]i$ resulting from addition of 1 mM extracellular Ca^{2+} (SRCE) in the experiment shown, calculated as area under the curve (integrated area) and by peak height (initial calcium entry). Data are presented as mean ± S.E.M. (n= 15-25 cells) and were analyzed by t-test. In all cases, significant differences between groups ($p<0.05$) are indicated by an asterisk (*). Data are representative of 3 independent experiments.

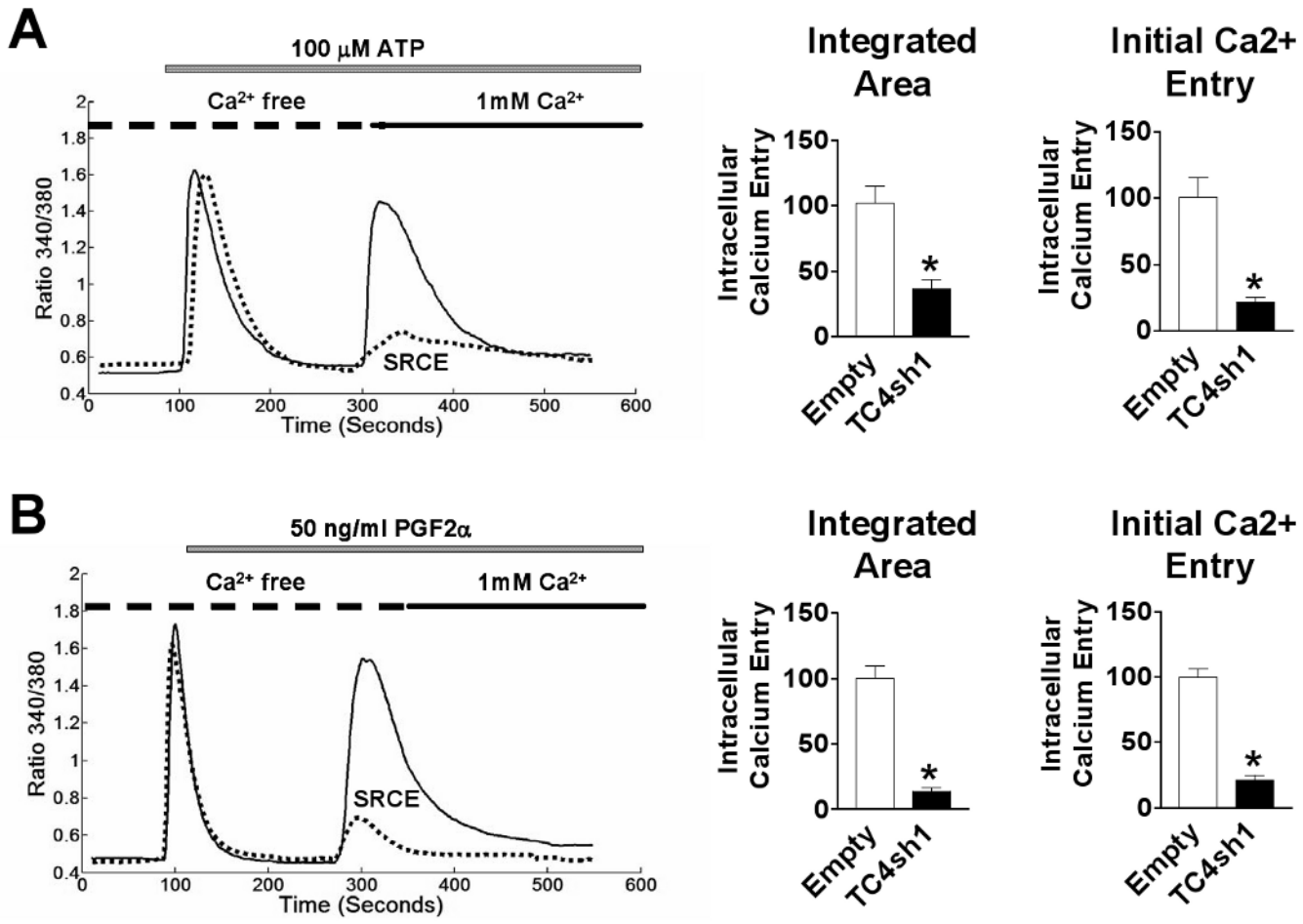

Fig. 6.

TRPC4 knockdown induces attenuation of other GPCR-stimulated SRCE. *Top*: SRCE induced by 100 μM ATP (A) and 50 ng/ml PGF2α (B) in PHM1-41 cells infected with empty adenovirus (solid lines) and cells infected with virus expressing TC4sh1 (dotted lines). *Bottom*: Mean changes in $[Ca^{2+}]_i$ resulting from addition of 1 mM extracellular Ca^{2+} (SRCE) in the experiment shown, calculated as area under the curve (integrated area) and by peak height (initial calcium entry). Data are presented as mean ± S.E.M. (n=35-45 cells) and were analyzed by t-test. In all cases, significant differences between groups ($p<0.05$) are indicated by an asterisk (*). Data are representative of 4 independent experiments.

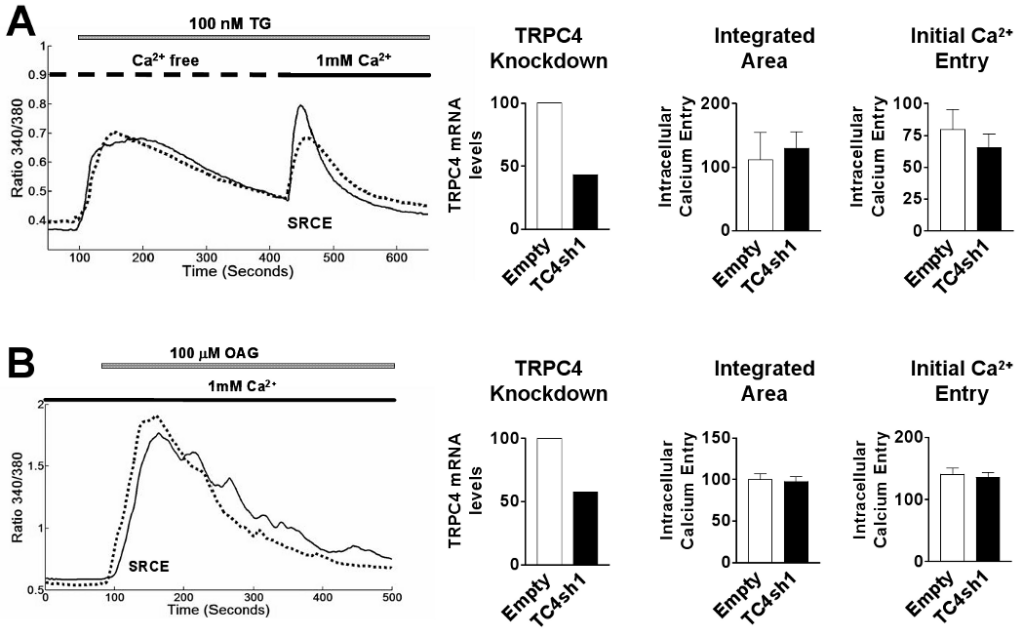

Fig.7.

Lack of effect of TRPC4 knockdown on TG- and OAG-stimulated SRCE. *Left*. SRCE induced by either (A) 100 nM TG and (B) 100 μM OAG in PHM1-41 cells infected with empty adenovirus (solid lines) and cells infected with virus expressing TC4sh1 (dotted lines). *Middle*. TRCP4 mRNA levels expressed relative to empty vector in the experiment shown. *Right*: Mean changes in $[Ca^{2+}]_i$ resulting from addition of 1 mM extracellular Ca^{2+} (SRCE) in the experiment shown, calculated as area under the curve (integrated area) and peak height (initial calcium entry) (n=45-55 cells). Data are presented as mean ± S.E.M. and were analyzed by t-test. In all cases, significant differences between groups ($p<0.05$) are indicated by an asterisk (*). Data are representative of 10 and 7 independent experiments for TG and OAG, respectively.

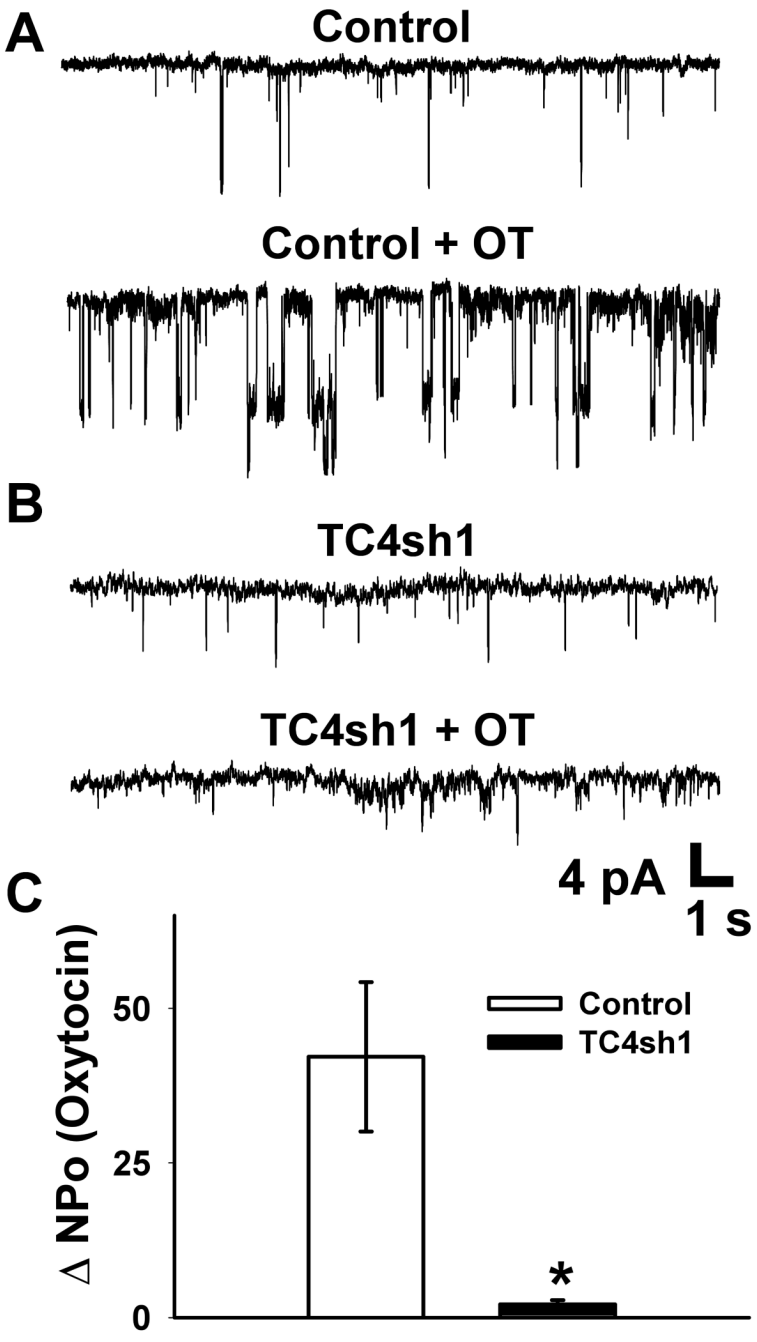

Fig. 8.

Activation of cation currents by oxytocin in PHM1-41 cells was attenuated by the expression of TC4sh1. (A) Representative trace of single-channel cell-attached recordings from PHM1-41 cells infected with empty vector *(top)*, and in response to 100 nM oxytocin *(bottom)*. (B) Representative trace of single-channel cell-attached recordings from PHM1-41 cells infected with adenovirus expressing TC4sh1 for >72 h *(top)*, and in response to oxytocin *(bottom)*. (C) Summary of the change in total open probability (ΔNP_o) in response to administration of oxytocin for control (n=5) and TC4sh1 (n=5) treated PHM1-41 cells. Data are presented as mean ± S.E.M. and were analyzed by t-test. The difference between the two groups was significant at ($p<0.05$) and is indicated by an asterisk (*).

Table 1

Short-hairpin RNA (shRNA) sequences for targeting TRPC4 mRNA and PCR primers

Target	Orientation	oligonucleotide sequence (5′-3′)
TC4sh1 shRNA	Forward	5′GCG**CATGTTGGAGATGCTCTATTAC**CTGTGAAGCCACAGATGGG**GTAATAGAGCATCTCCAACATA**TGCTTTTTT3′
	Reverse	5′*GATC*AAAAAAGCA**TATGTTGGAGATGCTCTATTAC**CCCATCTGTGGCTTCACAG**GTAATAGAGCATCTCCAACATG**CGCC
TC4sh2 shRNA	Forward	5′GCG**AAGGTGCCTCCTATACTCCTTG**CTGTGAAGCCACAGATGGG**CAAGGAGTATAGGAGG CACCTG**TGCTTTTTT3′
	Reverse	5′*GATC*AAAAAAGCA**CAGGTGCCTCCTATACTCCTTG**CCCATCTGTGGCTTCACAG**CAAGGAGTATAGGAGGCACCTT**CGC
TC4sh3 shRNA	Forward	5′GCG**AAGACGAGAAGTTCCAGAGAAC**CTGTGAAGCCACAGATGGG**GTTCTCTGGAACTTCT CGTCTG**TGCTTTTTT3′
	Reverse	5′*GATC*AAAAAAGCA**CAGACGAGAAGTTCCAGAGAAC**CCCATCTGTGGCTTCACAG**GTTCTCTGGAACTTCTCGTCTT**CGC
TC4sh4 shRNA	Forward	5′GCG**AAACTGATTGCTGACCATGCAG**CTGTGAAGCCACAGATGGG**CTGCATGGTCAGCAATCAGTTG**TGCTTTTTT3′5′*GA*
	Reverse	**ACCATGCAG**CCCATCTGTGGCTTCACAG**CTGCATGGTCAGCAATCAGTTT**CGC*CG* 3′
shx1 shRNA	Forward	5′GCG**CGTAGTAATGACAATCCGCGCT**CTGTGAAGCCACAGATGGG**AGCGCGGATTGTCATT ACTACT**TGCTTTTTT3′
	Reverse	5′*GATC*AAAAAAGCA**AGTAGTAATGACAATCCGCGCT**CCCATCTGTGGCTTCACAG**AGCGCGGATTGTCATTACTACG**CGC
TRPC4	Forward	5′-TCAGACTTGAACAGGCAAGGTCCA-3′
PCR	Reverse	5′-AGTCCGCCATCCCACATCTGTTTA-3′
GUS	Forward	5′-GGCTTCGAGGAGCAGTGGTAC-3′
PCR	Reverse	5′-TGTCATTGAAGCTGGAGGGAAC-3′
PMCA1	Forward	5′-GGGTGGGAGAAATGAACTGA-3′
PCR	Reverse	5′-CTCTCTCCCATCCAGGACTG-3′
PMCA4	Forward	5′-CAATGCGGTGGATTGCAAAGT-3′
PCR	Reverse	5′-AACACAGCAGCTGACGTGACAATG-3′
SERCA2	Forward	5′-TGCTGTTGGTGACAAAGTTCCTGC-3′
PCR	Reverse	5′-TATCTTGGTTGACAGCTCGTGGGT-3′

shRNA target sequences for TRPC4 (in bold) were incorporated into the human miR-30 pre-micro RNA (pre-miRNA) backbone. Bases in italics were used for cloning of shRNA construct into the pSHAG vector. PMCA1, PMCA4 and SERCA2 primers detect both a and b isoforms.